Journal of Atmospheric and Solar-Terrestrial Physics 170 (2018) 1–10

Contents lists available at ScienceDirect

Journal of Atmospheric and Solar-Terrestrial Physics

journal homepage: www.elsevier.com/locate/jastp

Assessment of the NeQuick-2 and IRI-Plas 2017 models using global and long-term GNSS measurements

Daniel Okoh [a,b,*], Sylvester Onwuneme [c], Gopi Seemala [b], Shuanggen Jin [d], Babatunde Rabiu [a], Bruno Nava [e], Jean Uwamahoro [f]

[a] Center for Atmospheric Research, National Space Research and Development Agency, Nigeria
[b] Indian Institute of Geomagnetism, Navi Mumbai, India
[c] Department of Physics, University of Port Harcourt, Nigeria
[d] Shanghai Astronomical Observatory, Chinese Academy of Sciences, Shanghai 200030, China
[e] Abdus Salam International Center for Theoretical Physics, Trieste, Italy
[f] Department of Mathematics and Science, University of Rwanda, Kayonza, Rwanda

ARTICLE INFO

Keywords:
TEC
NeQuick-2
IRI-Plas 2017
GNSS

ABSTRACT

The global ionospheric models NeQuick and IRI-Plas have been widely used. However, their uncertainties are not clear at global scale and long term. In this paper, a climatologic assessment of the NeQuick and IRI-Plas models is investigated at a global scale from global navigation satellite system (GNSS) observations. GNSS observations from 36 globally distributed locations were used to evaluate performances of both NeQuick-2 and IRI-Plas 2017 models from January 2006 to July 2017, covering more than the 11-year period of a solar cycle. An hourly interval of diurnal profiles computed on monthly basis was used to measure deviations of the model estimations from corresponding GNSS VTEC observations. Results show that both models are fairly accurate in trends with the GNSS measurements. The NeQuick predictions were generally better than the IRI-Plas predictions in most of the stations and the times. The mean annual prediction errors for the IRI-Plas model typically varied from about 3 TECU at the high latitude stations to about 12 TECU at the low latitude stations, while for the NeQuick the values are respectively about 2–7 TECU. Out of a total 4497 months in which GNSS data were available for all the stations put together for the entire period covered in this work, the NeQuick model was observed to perform better in about 83% of the months while the IRI-Plas performed better in about 17% of the months. The IRI-Plas generally performed better than the NeQuick at certain locations (e.g. DAV1, KERG, and ADIS). For both models, the most of the deviations were witnessed during local daytimes and during seasons that receive maximum solar radiation for various locations. In particular, the IRI-Plas model predictions were improved during periods of increased solar activity at the low latitude stations. The IRI-Plas model overestimates the GNSS VTEC values, except during high solar activity years at some high latitude stations. The NeQuick underestimates the TEC values during the high solar activity years and overestimates it during local daytime for low and moderate solar activity years, but not as much as the IRI-Plas does.

1. Introduction

The ionosphere affects *trans*-ionospheric radio propagations. The evolution of our navigation requirements into satellite based systems is also adding a rapid stair to our interest in ionospheric research since the ionosphere is the major source of error for our satellite based navigation systems (e.g., Jin et al., 2004, 2006, and 2007; Jin and Najibi, 2014). The greatest efforts in ionospheric research have been directed towards ionospheric modeling and related studies that tend to understand how the ionosphere changes in time and space. Several models of the ionosphere have been developed (e.g. Chiu, 1975; Roble et al., 1988; Bilitza, 1990; Bailey et al., 1997; Huba et al., 2000; Habarulema, 2010; Okoh et al., 2016).

Ionospheric models are useful when it comes to forecasting and predicting the behavior of the ionosphere for locations and time instances where empirical observations are not available. A major concern for users of ionospheric models is to understand how accurate the models predict required ionospheric parameters. A subtle approach to evaluating the

* Corresponding author. Center for Atmospheric Research, National Space Research and Development Agency, Nigeria.
E-mail address: okodan2003@gmail.com (D. Okoh).

https://doi.org/10.1016/j.jastp.2018.02.006
Received 11 December 2017; Received in revised form 26 January 2018; Accepted 18 February 2018
Available online 22 February 2018
1364-6826/

performance of the models has always been to compute the model errors by comparing the model predictions with corresponding observations from equipment. This practice is also popular among ionospheric scientists (e.g. Buresova et al., 2006; Jin and Park, 2007; McKinnell et al., 2007; Rabiu et al., 2011, 2014; Okoh et al., 2012, 2015; Ezquer et al., 1994, 2017) who have interests in either assessing the model performances to improve them or assessing/validating the models for other applications.

Following the rapid proliferation of GNSS receivers over the past decade, they have become popular sources of ionospheric information. The total electron content (TEC) is the most dominant ionospheric component that affects GNSS signal propagations (Klobuchar, 1996; Seemala and Delay, 2010). The basic principle behind the use of GNSS receivers as sources of ionospheric information is that when GNSS signals transverse the ionosphere, the signals suffer time delays by amounts which are directly proportional to the TEC along the signal path, and inversely proportional to the squares of the signal frequencies. Dual (or more) frequency GNSS receivers are therefore able to compute TEC from the differential delay information they get from different-frequency radio signals.

The International Reference Ionosphere (IRI) model (Bilitza, 1990) is one of the most popular ionospheric models. The model has been widely accepted as a defector standard for specifying ionospheric parameters across the globe. Perhaps, the most discussed limitation about the model, especially for researchers interested in comparing the model predictions with GNSS observations, is that it computes ionospheric parameters only up to altitudes of 2000 km (Gulyaeva and Bilitza, 2012; Maltseva et al., 2013; Okoh et al., 2015; Arikan et al., 2016; Ezquer et al., 2017). The TEC computed by GNSS receivers involves electron density integrations up to the height of the GNSS satellites (about 20200 km), whereas this is only up to a maximum of 2000 km for the IRI model. This makes it difficult to comprehensively assess the IRI-TEC predictions using TEC computed from the GNSS. To overcome this rigor, we have opted to use the IRI-Plas model (the IRI extended to the plasmasphere; Gulyaeva et al., 2002) which has also been proposed for extension of the IRI model to the plasmasphere (Gulyaeva and Bilitza, 2012).

The NeQuick (Hochegger et al., 2000; Radicella and Leitinger, 2001; Nava et al., 2008) is another popular global ionospheric model which has been severally compared with GNSS TEC measurements and shown to be a good representation of the ionosphere (Jodogne et al., 2005; Bidaine and Warnant, 2010; Wang et al., 2017; Ezquer et al., 2017). The NeQuick was first developed based on the DGR profiler (proposed by Di Giovanni and Radicella (1990), and therefore the name DGR) and subsequently modified by Radicella and Zhang (1995). A new version of the NeQuick (the NeQuick 2) was developed by implementing further improvements by Radicella and Leitinger (2001), a modified bottomside introduced by Leitinger et al. (2005), and a modified topside proposed by Coïsson et al. (2006). The NeQuick is admired because of its improved performance in predicting the topside ionosphere, and consequently versions of the IRI model from 2007 and later have included the topside formulation of the NeQuick, and has adopted it as the most mature of the different proposals to compute the topside part of the IRI electron density profile (Bilitza and Reinisch, 2008; Nava et al., 2008; Okoh et al., 2015). The NeQuick includes routines that compute the electron density along any ray-path from ground to GNSS satellite altitudes of about 20200 km, and so it is appropriate, and eases comparison with GNSS measurements. Version 1 of the NeQuick was adopted by International Telecommunication Union Radio communication sector (ITU-R) as a procedure for estimating TEC, and the NeQuick2 is the one currently recommended by the ITU (Nava and Radicella, 2014). The latest version of the NeQuick is the NeQuick2, and this is the version that has been used in this work.

This work is the first to comprehensively assess the performances of both the NeQuick and the IRI-Plas model at a global scale as well as on a long-term basis. This is relevant to present a broad picture of the model performances in parts of the globe, and to understand how these performances vary with seasons and with various degrees of solar activity.

2. Data and methods

GNSS data used in this work was obtained from the University of California, San Diego (UCSD) network of GNSS receivers (http://garner.ucsd.edu/pub/). Data from a total of 36 globally-distributed GNSS receiver stations (Fig. 1) was used. Table 1 is a listing of all the 36 stations and their locations. The globe was divided into 6 longitudinal zones (from −180° to +180° in steps of 60°) and 6 latitudinal zones (from −90° to +90° in steps of 30°) forming a mesh grid of 36 cells as illustrated in Fig. 1. Each of the 36 stations were chosen from the UCSD network using the following criteria: (i) one station has to be selected from each of the grid cells, (ii) the stations, within each grid, having the most of available data were considered, and (iii) among the considered stations, the one that is closest to the center of the grid cell was chosen. In this paper, the six longitudinal zones shall respectively (from left to right) be referred to as the Pacific sector, the American sector, the Atlantic sector, the African sector, the Asian sector, and the Australian Sector. Similarly, the six latitudinal zones shall respectively (from top to bottom) be referred to as the Northern high latitude, the Northern middle latitude, the Northern low latitude, the Southern low latitude, the Southern middle latitude, and the Southern high latitude. All available data from each of the 36 receiver stations, covering the periods from January 2006 to July 2017, were used. Data obtained from the UCSD network were in RINEX format, and the RINEX data were processed into vertical TEC (vTEC) information using the most recent version of the GPS-TEC analysis application software (version 2.9.5) developed by Gopi Seemala. The software computes TEC based on the basic principle that two different-frequency GNSS signals transmitted at the same time from the same satellite through the same route will be differently delayed by the ionosphere. Rama Rao et al. (2006) and Seemala and Valladares (2011) contain the procedures used by the software to derive TEC information from the RINEX files. To reduce multipath errors, TEC information obtained from satellites with elevation angles less than 30° were excluded. For receivers in the Polar Regions, there are fewer number of GNSS satellites above the 30° mask, but since averages are taken over longer time spans, an adequate number of observations is accumulated, and better still, the results get more accurate by using the most reliable data sets. To further reduce the data, and to make the VTEC profiles smoother, the VTECs computed from the RINEX files were averaged in 1 h intervals. Finally, the monthly median values of the diurnal GNSS VTEC profiles were computed. This is necessary because the NeQuick and IRI-Plas models used in this work are monthly average representations of the ionosphere, and also computing the monthly median values will eliminate large VTEC deviations which are associated with events like geomagnetic storms.

Corresponding monthly VTEC values were obtained from the NeQuick-2 using the windows executable program created from the FORTRAN source code which was obtained from the Ionosphere Radio propagation Unit of the T/ICT4D Laboratory (https://t-ict4d.ictp.it/

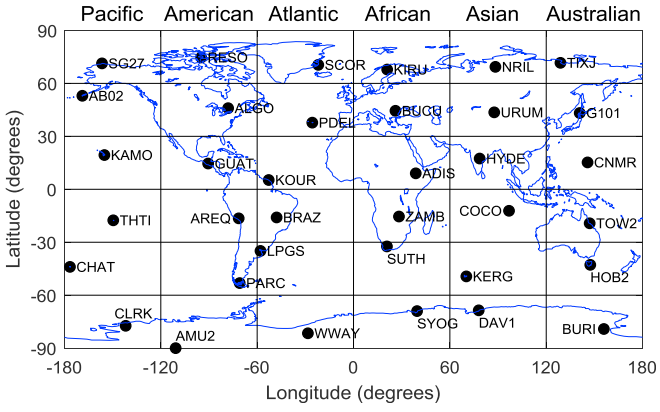

Fig. 1. Distribution of GNSS receiver locations used in this work.

Table 1
List of 36 GNSS receiver stations used in this work.

Station ID	City	Country	Geographic Latitude	Geographic Longitude	Altitude (m)
ADIS	Addis Ababa	Ethiopia	9.0	38.8	2439.2
ZAMB	Lusaka	Zambia	−15.4	28.3	1324.9
BUCU	Bucuresti	Romania	44.5	26.1	143.2
SUTH	Sutherland	South Africa	−32.4	20.8	1799.8
KIRU	Kiruna	Sweden	67.9	21.0	391.1
SYOG	East Ongle Island	Antarctica	−69.0	39.6	50.1
KOUR	Kourou	French Guiana	5.3	−52.8	−25.6
BRAZ	Brasilia	Brazil	−15.9	−47.9	1106.0
PDEL	Ponta Delgada	Portugal	37.7	−25.7	110.8
LPGS	La Plata	Argentina	−34.9	−57.9	29.9
SCOR	Scoresbysund	Denmark	70.5	−22.0	128.5
WWAY	Whichaway	Antarctica	−81.6	−28.4	1195.4
HYDE	Hyderabad	India	17.4	78.6	441.7
COCO	Cocos Island	Australia	−12.2	96.8	−35.2
URUM	Urumqi	China	43.6	87.6	856.1
KERG	Port aux Francais	French Southern Territories	−49.4	70.3	73.0
NRIL	Norilsk	Russia	69.4	88.4	47.9
DAV1	Davis	Antarctica	−68.6	78.0	44.5
GUAT	Guatemala City	Guatemala	14.6	−90.5	1519.9
AREQ	Arequipa	Peru	−16.5	−71.5	2488.9
ALGO	Algonquin-Park	Canada	46.0	−78.1	202.0
PARC	Punta Arenas	Chile	−53.1	−70.9	22.3
RESO	Resolute	Canada	74.7	−94.9	34.9
AMU2	South Pole	Antarctica	−90.0	−110.8	2823.0
CNMR	Saipan	United States	15.2	145.7	64.4
TOW2	Cape Ferguson	Australia	−19.3	147.1	88.2
G101	Otaru	Japan	43.2	140.9	38.4
HOB2	Hobart	Australia	−42.8	147.4	41.1
TIXJ	Tixi	Russia	71.6	128.9	47.1
BURI	Butcher Ridge	Antarctica	−79.1	155.9	2007.0
KAMO	Hawaii	United States	19.4	−155.1	780.8
THTI	Papeete	French Polynesia	−17.6	−149.6	98.5
AB02	Nikolski	United States	53.0	−168.9	192.8
CHAT	Waitangi	New Zealand	−44.0	−176.6	58.0
SG27	Barrow	United States	71.3	−156.6	9.4
CLRK	Clarke Mountains	Antarctica	−77.3	−141.9	1000.9

nequick2/source-code). Also, corresponding monthly VTEC values were obtained from the IRI-Plas 2017 model using the windows executable program which was obtained from the website of the IZMIRAN Institute (http://ftp.izmiran.ru/pub/izmiran/SPIM/). One important update to the IRI-Plas 2017 version is the inclusion of 8 options of solar proxy indices for user-selection. Results obtained from the model will differ depending on which of the 8 options is used. A major idea in this work is to motivate lowering of the model prediction errors based on their default settings. Therefore, option number 1 (SSN1 and F10.7), which is default for the model, was used.

To measure the error (or difference) between a model prediction and the corresponding GNSS observation, we compute the VTEC deviations simply as the model prediction value minus the corresponding GNSS observation value. To further make a comparative study of the two models over long time, and to investigate exactly how close the model values are to the GNSS observations at the various locations, we further compute the root-mean-square of the monthly median diurnal profiles of the VTEC deviations using the formula in equation (1). This value (which we shall henceforth refer to as the monthly RMSD) gives a sense, on the average, of the typical error between a model prediction and the corresponding GNSS observation for the month.

$$\text{Monthly RMSD} = \sqrt{\frac{\sum_{i=1}^{n} \Delta T_i^2}{n}} \tag{1}$$

$\Delta T_i s$ are VTEC deviations of the model predictions from corresponding GNSS observations at hourly time instances (i). n is the number of diurnal hours (typically 24 for a complete profile).

3. Results and discussions

Fig. 2(a)–(d) illustrate how the VTEC predictions from the IRI-Plas and the NeQuick compare with the GNSS VTEC observations. The figures represent monthly median diurnal profiles for the month of March and for years 2006, 2009, 2012, and 2014 respectively. Years 2009, 2012, and 2014 were chosen to respectively represent years of low, moderate, and high solar activity. The figures are made up of 36 panels arranged in a 6-by-6 subplot structure. Each of the 36 panels contains the plot for each of the 36 stations considered in this work. The subplot structure is designed to depict the spatial locations of the stations as shown in the world map of Fig. 1. The empty panels indicate that there are no available GNSS data for the particular stations represented. Results for the month of March are arbitrarily chosen for illustration since it will be ambiguous to attempt an illustration with all months in a year. A more concise monthly treatment is however included in a later part of this paper.

Fig. 3(a)–(f) were constructed to investigate the performance of the models according to the months/seasons and local times. The figures represent the model VTEC deviations from corresponding GNSS values (computed by subtracting the GNSS values from the corresponding model values, so that positive values indicate that the models overestimate the GNSS values while negative values indicate that the models underestimate the GNSS values). As shown on the color bar, the darker blue colors indicate more under estimations while the darker red colors indicate more over estimations. The green colors indicate zero (or close to zero) deviations and as such depict the more accurate predictions. Fig. 3(a)–(f) are respectively the VTEC deviations for the Pacific, American, Atlantic, African, Asian, and Australian sectors for year 2012. Year 2012 was arbitrarily chosen, also considering it is a year of moderate solar activity.

Using the formula in equation (1), we compute and illustrate the typical monthly errors of the model predictions for years 2009 and 2014 as shown in Fig. 4(a)–(f). Again the two years were selected to represent years of low and high solar activities respectively. And the figures respectively illustrate results for the six longitudinal zones in this work. To investigate and make long-term comparisons of the two models, we compute and illustrate the annual mean of the monthly RMSDs for all the years from 2006 to 2017. Fig. 5(a) is a summary of the mean annual RMSDs for all 36 stations used in this study, while Fig. 5(b) is a reconstruction of Fig. 5(a) as a function of the percentage annual RMSDs (rather than as a function of the mean annual RMSDs).

Fig. 6(a) is a surface plot that shows how the monthly RMSDs for the IRI-Plas vary over all months and all years used in this work for all the 36 stations. Fig. 6(b) is an equivalent plot for the NeQuick. Fig. 6(c) and (d) are respectively corresponding percentage monthly RMSD plots for the IRI-Plas and the NeQuick. Fig. 7 is a summary of the instances and locations when either the NeQuick or the IRI-Plas predictions are better. The red patches indicate instances and locations when the NeQuick is better than the IRI-Plas, while the blue patches indicate instances and locations when the IRI-Plas is better than the NeQuick. The white patches are instances when there are no available GNSS data for the stations.

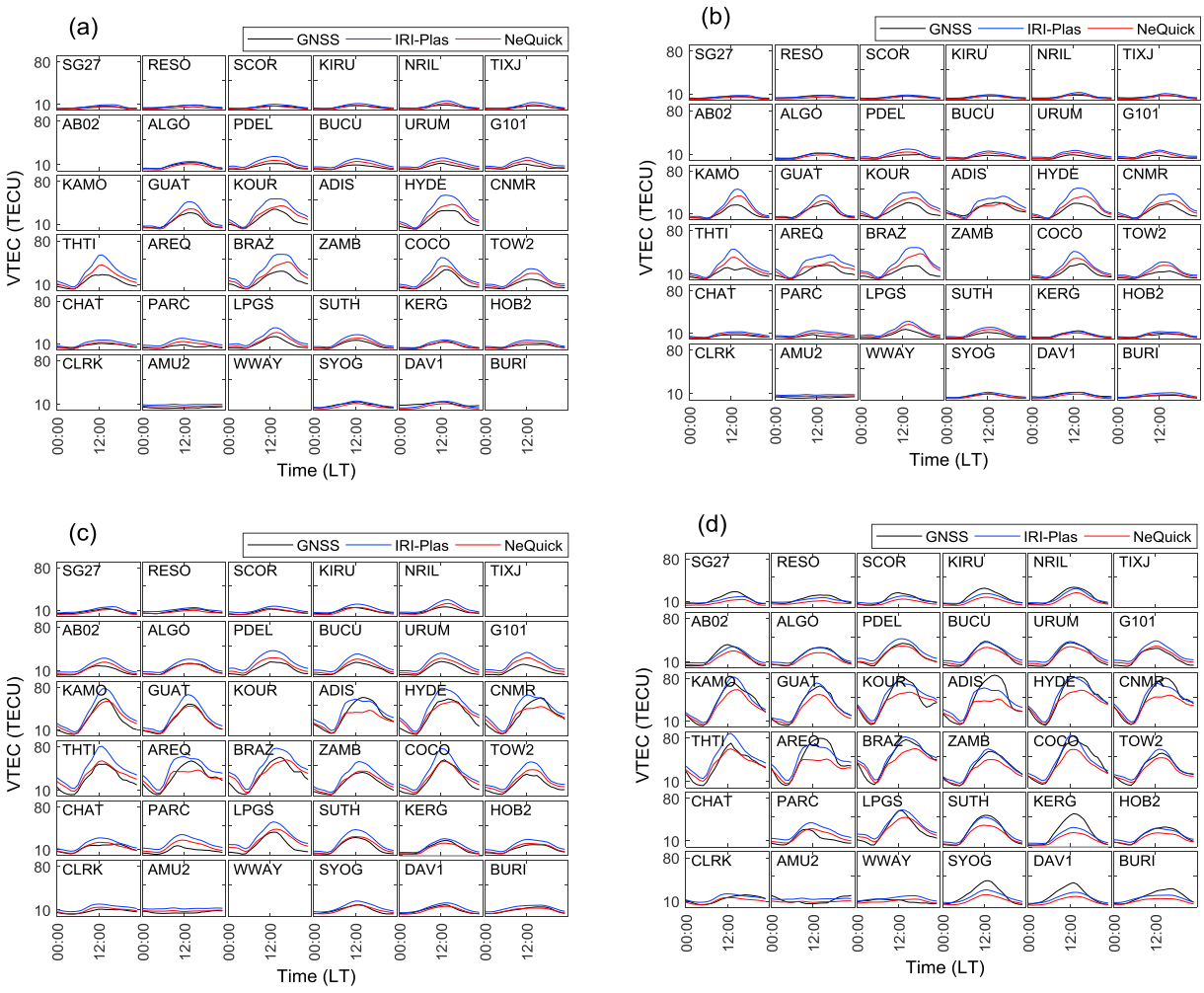

Fig. 2. Monthly median diurnal VTEC profiles for March (a) 2006, (b) 2009, (c) 2012, and (d) 2014.

3.1. Mean biases

Fig. 2(a)–(d) reveal that VTEC predictions from both models generally correlate well with the GNSS VTEC observations. There is a clear indication that the IRI-Plas model typically overestimates the GNSS VTEC (especially during the local daytimes) in almost all of the 36 stations. Fig. 3(a)–(f) show that the VTEC deviations for both models are generally in the range of ±20 TECU. The figures show that most of the overestimations come from the IRI-Plas while most of the underestimations come from the NeQuick. The greatest overestimations of about 20 TECU are seen for the IRI-Plas at the low latitude stations and around local middays, while the greatest underestimations (also of about 20 TECU) are seen for the NeQuick at the low latitude stations of ADIS, AREQ, CNMR, HYDE and COCO (also around local midday). Underestimations of about 20 TECU are also observed for the NeQuick at all southern stations in the Asian sector.

Fig. 4(a)–(f) show that typical monthly RMSDs are less than 5 TECU for both models at the high latitude stations. The values get around 5 to 10 TECU for the middle latitude stations, and greater than 10 TECU for low latitude stations, with the IRI-Plas showing most of the higher deviations. The best case scenario for the NeQuick was in year 2009 at the Australian high latitude station of BURI where the monthly RMSDs were less than 2 TECU for all the months in that year. The best case scenario for the IRI-Plas was also in year 2009 at the Asian middle latitude station of KERG where the monthly RMSDs were also less than 2 TECU for all the months in that year (except for the months of November and December when the values were respectively 2.1 and 2.6 TECU). The values were even less than 1 TECU for the months of February, March, September and October. The IRI-Plas monthly RMSDs were also less than 2 TECU at the Asian Northern high latitude station of NRIL for all the months in year 2009 when there were available GNSS observations for the station. The worst case scenario for the NeQuick was in year 2014 at the African low latitude station of ADIS when the monthly RMSD reached 21 TECU for the month of March. For the IRI-Plas, the worst case scenario was in year 2009 at the Atlantic low latitude station of BRAZ when the monthly RMSDs were about 20 TECU in the months of March and October. Fig. 5(a) shows that the typical mean annual errors for the IRI-Plas predictions increase from about 3 TECU at the high latitudes to about 12 TECU at the low latitudes. For the NeQuick, the mean annual errors increase from about 2 TECU at the high latitudes to about 7 TECU at the low latitudes.

3.2. Diurnal variations

Figs. 2 and 3 clearly indicate that (for both NeQuick and IRI-Plas) the most of the VTEC deviations are observed during the local daytimes as compared to nighttime and early morning values. There is a generally expected behavior for models to predict smaller-valued quantities with better accuracies; systematically, larger-valued quantities will lead to larger errors. The solar-zenith angle during local daytimes are smaller than at night and early morning times, and since the Sun is the major source of ionospheric ionization, the daytime VTEC values are higher than nighttime and early morning values. Consequently the errors in predicting daytime values are systematically larger than in predicting

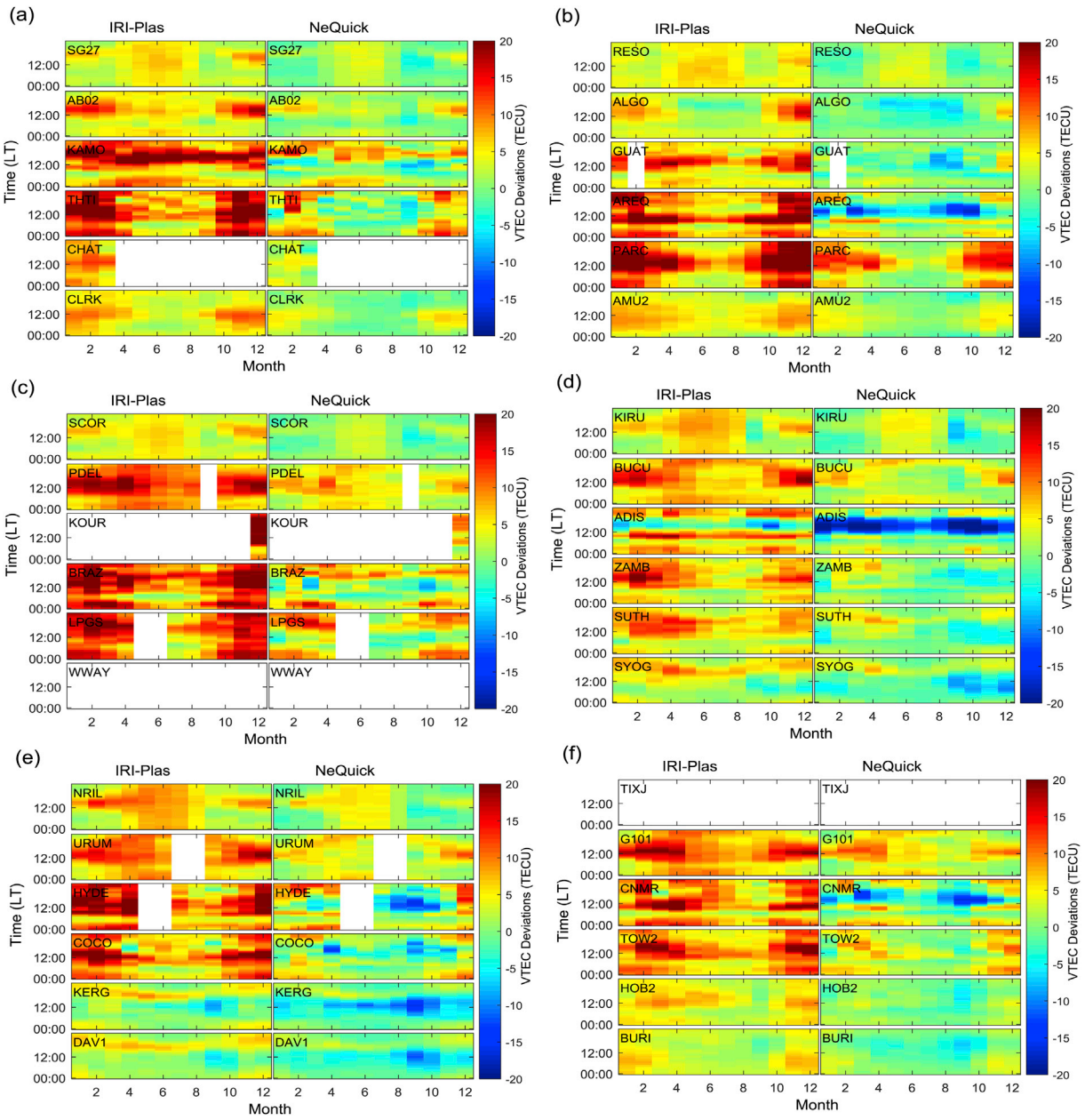

Fig. 3. VTEC Deviations for year 2012 of (a) the Pacific sector stations, (b) the American sector stations, (c) the Atlantic sector stations, (d) the African sector stations, (e) the Asian sector stations, and (f) the Australian sector stations.

nighttime and early morning values.

Figs. 2 and 3 also predominantly show that the IRI-Plas overestimates the GNSS VTEC especially during the local daytimes. Other studies (e.g. Zakharenkova et al., 2015; Adebiyi et al., 2016; Ezquer et al., 2017) also show that the IRI-Plas model overestimates GNSS TEC observations during the local daytimes. In comparing the IRI-Plas to the NeQuick, Ezquer et al. (2017) opined that one of the reasons for the overestimation of the IRI-Plas could be due to erroneous prediction of the plasmaspheric contribution to the vertical total electron content. While we understand that this inclusion obviously increases the values of the IRI-Plas VTEC predictions, we reason that the results from studies as this one could be helpful to strategically improve predictions of the IRI-Plas model. A core idea in this study is therefore to present the results in a manner that can be utilized to improve the TEC predictions of both models in future.

Fig. 3 reveals that there are more cases of local daytime underestimations of the GNSS VTEC by the NeQuick than the cases of local daytime overestimations. There are however some cases of local daytime overestimations by the NeQuick, but the deviations are not as high as with the IRI-Plas. The worst case of local daytime underestimations are observed for the NeQuick at the African low latitude station of ADIS, while the worst case of local daytime overestimations are observed for the IRI-Plas at the Pacific low latitude station of KAMO. There are some other intense cases of overestimations by the IRI-Plas that span into the local nightimes, but these cases are not as continuous throughout the year as with the KAMO station. There are very few cases of local daytime underestimations of the GNSS VTEC by the IRI-Plas (e.g. at the African low latitude station of ADIS), and also some cases of local daytime overestimations of the GNSS VTEC by the NeQuick (e.g. the middle latitude stations of PDEL and G101).

3.3. Latitudinal and longitudinal variations

It is also clearly evident from Figs. 2 and 3 that the most of VTEC deviations are witnessed in the low latitudes as compared to the middle

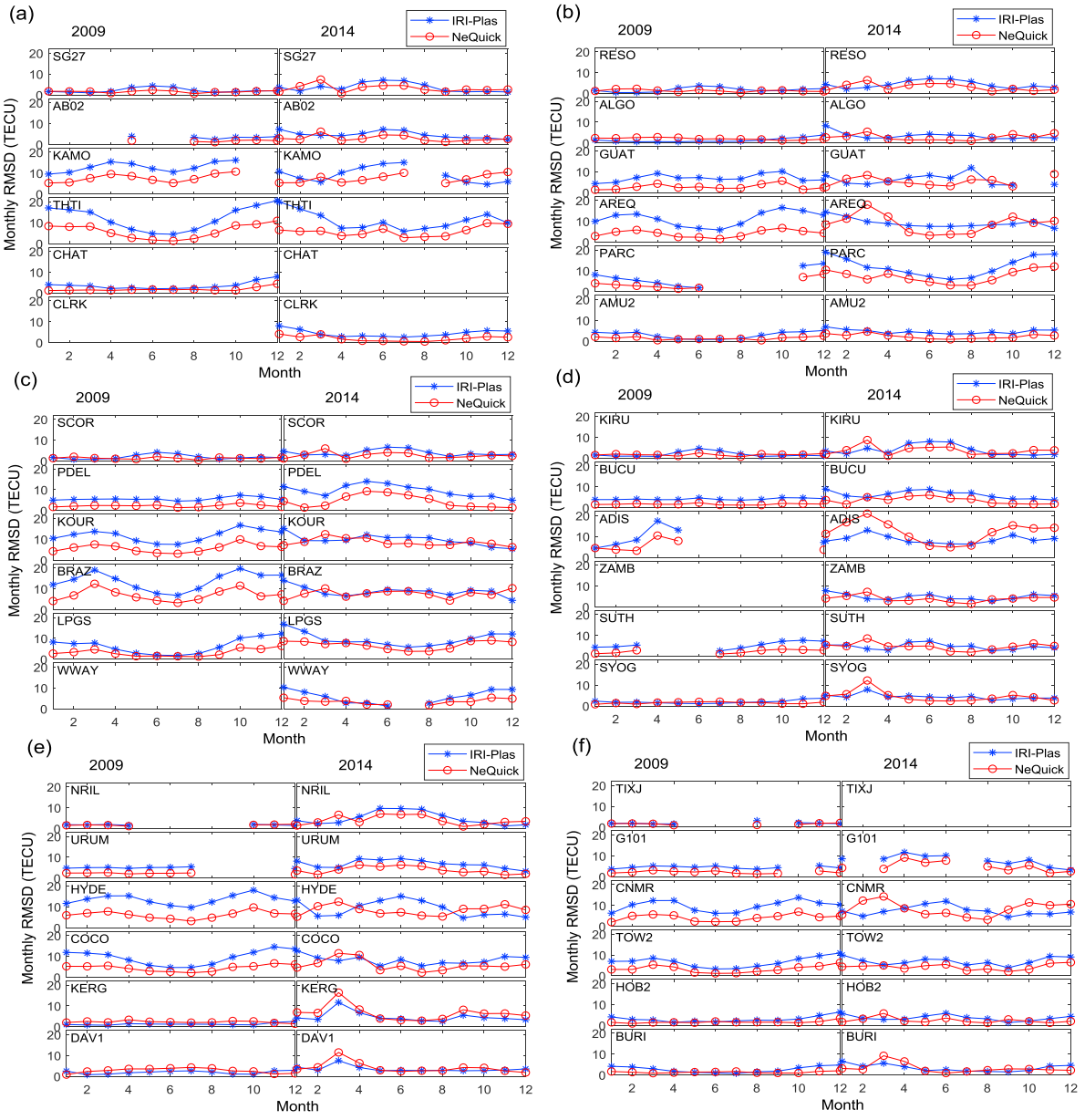

Fig. 4. Monthly RMSDs for (a) the Pacific sector stations, (b) the American sector stations, (c) the Atlantic sector stations, (d) the African sector stations, (e) the Asian sector stations, and (f) the Australian sector stations.

and the high latitudes. In a similar explanation as used for the diurnal variations, the VTEC values are known to be generally higher in the low latitudes than in the middle and high latitudes. One obvious reason is the proximity to sunlight of ionizable matter in the low latitudes as compared to the middle and high latitudes. The mean solar-zenith angle is also least at the low latitudes compared to the middle and high latitudes, and so the low latitudes more often receive direct solar radiation impact than the other latitudinal regions. The solar radiation impact reduces as one move from the low latitudes through the middle latitudes to the high latitudes. Since the VTEC values are greater at the low latitudes, the accompanying error in their prediction is also greater, and so the model predictions of the values deviate more than as compared to the middle and high latitudes.

Apart from the systematically increased VTEC magnitudes at the low latitudes, the region (especially around the geomagnetic equator) is prone to several anomalous ionospheric phenomena (e.g. occurrences of the equatorial ionization anomaly, scintillations and equatorial plasma bubbles) that make it difficult to model/characterize. This therefore also increases the model prediction errors for low latitudes, and also accounts for the greater deviations observed for the low latitude stations than for the middle and high latitudes.

Fig. 6 shows that the worst deviation cases for the IRI-Plas are on the Atlantic sector (with KOUR, BRAZ, and LPGS stations mostly affected). There are also large deviations observed for the American stations of AREQ and PARC, for the Pacific low latitude stations of KAMO and THTI, and for the Asian low latitude stations of HYDE and COCO. The worst deviation case for the NeQuick is on the African sector (with the low latitude station of ADIS mostly affected). Other large deviations are observed for the Atlantic stations of KOUR and BRAZ, for the American stations of AREQ and PARC, and for the Pacific low latitude stations of KAMO and THTI. These NeQuick deviations are however not as much as the IRI-Plas deviations.

Fig. 7 is presents a summary of the comparative analysis between both models for all the locations used in this study. The figure shows that the IRI-Plas is mostly better at the Asian middle and high latitude stations of KERG and DAV1, at the African low latitude stations of ADIS, and at

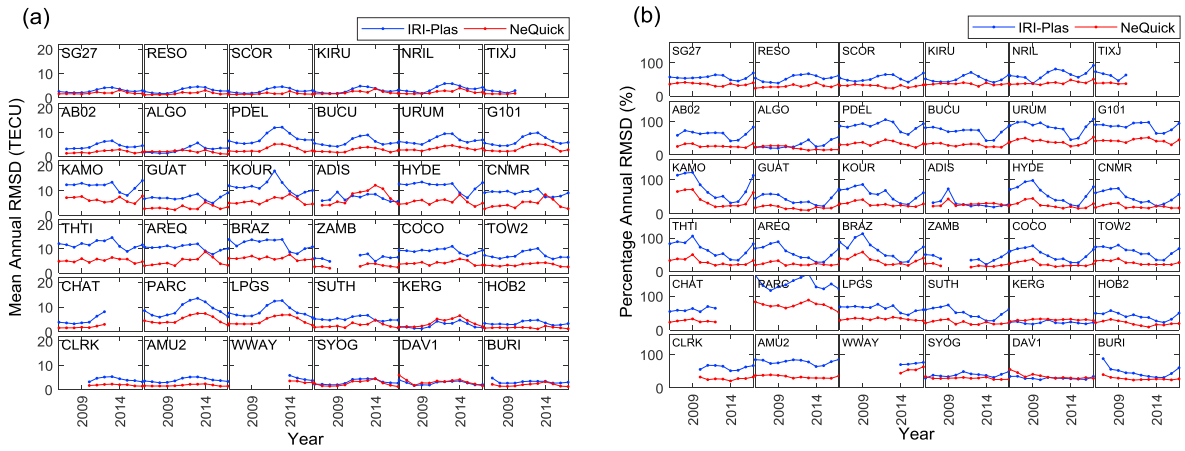

Fig. 5. (a) Mean Annual RMSDs, and (b) Percentage Annual RMSDs, for all stations used in this work. The horizontal axes run from 2006 to 2017 but for lack of space, 2009 and 2014 are shown to indicate low and high solar activity years.

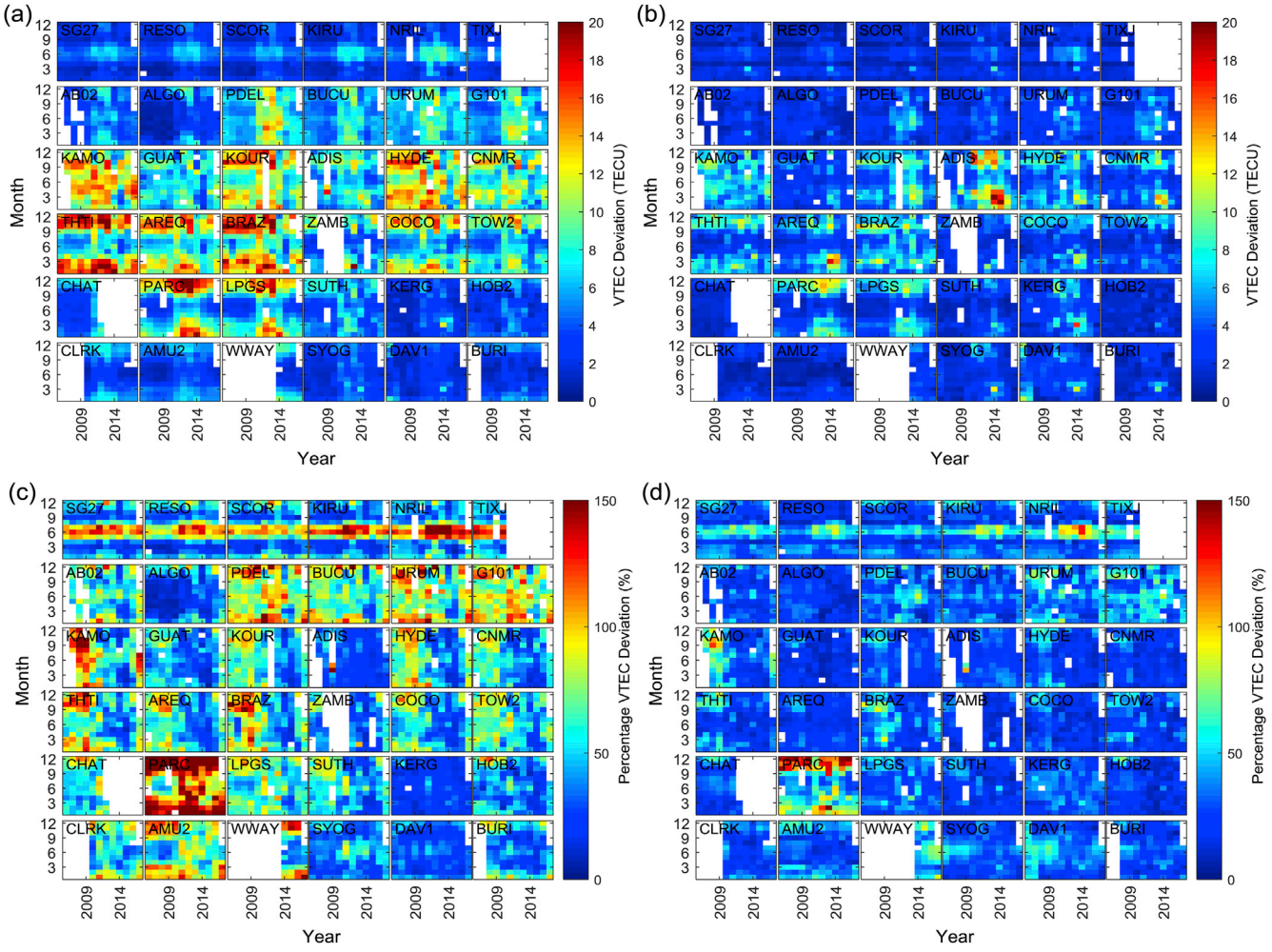

Fig. 6. Surface plots of (a) Monthly RMSD variations for the IRI-Plas, (b) Monthly RMSD variations for the NeQuick, (c) Percentage Monthly RMSDs for the IRI-Plas, and (d) Percentage Monthly RMSDs for the NeQuick.

the American middle latitude station of ALGO. The NeQuick is mostly better than the IRI-Plas at the rest of the other locations. Fig. 5 also shows that the NeQuick prediction errors are lower than the IRI-Plas prediction errors for most of the years and in most of the stations. The IRI-Plas model was also particularly observed to perform better than the NeQuick at the same two Asian sector stations of KERG and DAV1, and at the same African station of ADIS. In a related study, Bolaji et al. (2017) had shown that the IRI-Plas model appeared to be the best of all models (comprising the NeQuick and all 3 topside formulations IRI model) in predicting the TEC at equatorial ionization anomaly crest locations in the northern

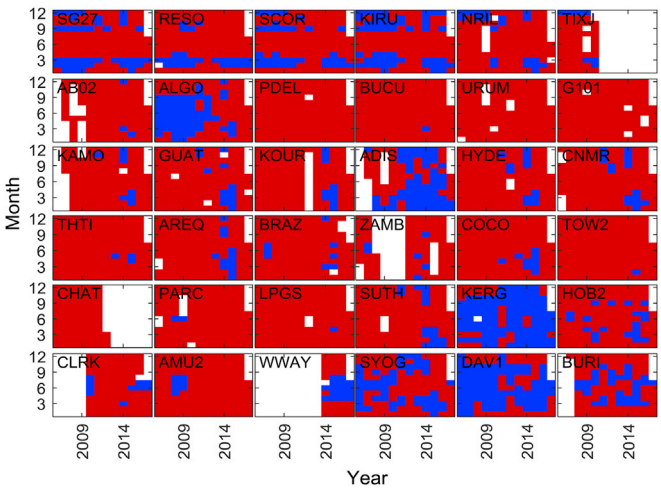

Fig. 7. Summary of instances and locations when either the NeQuick or the IRI-Plas predictions are better. The red patches indicate instances and locations when the NeQuick is better, while the blue patches indicate instances and locations when the IRI-Plas is better. The white patches are instances when there are no available GNSS data for the stations. (For interpretation of the references to color in this figure legend, the reader is referred to the Web version of this article.)

hemisphere of Africa.

3.4. Monthly and seasonal variations

Figs. 3, 4 and 6 indicate that the performances of the models vary with the months and with the seasons. Fig. 3 shows that at the low latitude stations, the VTEC deviations are greater during the equinox months (around the months of March and September) than during solstices (especially around the June Solstice). The contrast is observed for the high latitude stations. At the Northern high latitude stations, the VTEC deviations are greatest around the month of June (which is summer in the northern hemisphere), while at the Southern high latitudes the deviations are greatest around the months around December/January (which is summer in the southern hemisphere). Figs. 4 and 6 similarly show that the VTEC deviations are greater during the equinoxes (for the low latitude stations) and greater during the summer solstice months (for the high latitude stations). The VTEC values at the low latitude stations are enhanced during equinoxes following the decrease in mean solar-zenith angle at the low latitude region during equinoxes. The increased VTEC values at the region during equinoxes therefore systematically increases the model prediction errors during these seasons. In a similar explanation for the high latitude stations, the summer months are associated with enhanced VTEC values as compared to the winter months. During the summer months in either hemispheres, the hemispheres are more tilted towards the Sun, and as a result the mean solar-zenith angle is minimized for the hemispheres during the summer months. Consequently, the regions receive more direct impact of the solar radiation during these months, the ionospheric ionization (and hence VTEC) is increased, leading to systematically increased prediction errors by the models.

A somewhat consistent pattern that is observed in Fig. 7 is that, at the Northern high latitude stations, the IRI-Plas is observed to perform better the NeQuick during the months around February/March, and around the months of September and December. On the other hand, the NeQuick is observed to be consistently better at those stations around the months from April to August. For the American middle latitude station of ALGO (and in the years preceding year 2013), the IRI-Plas is observed to perform better than the NeQuick in most of the months from January to September, while the NeQuick performs better in most of the remaining months. In the summary of Fig. 7, there were a total of 4497 months in which GNSS data was available for all the stations put together. Out of this number, the NeQuick model performed better in 3740 months (representing 83% of the months) while the IRI-Plas performed better in 757 months (representing 17% of the months).

3.5. Long-time variations

Fig. 4 shows that the NeQuick prediction errors are dominantly lower than the IRI-Plas prediction errors in all the low latitude stations during the low solar activity year. One of the instances when the IRI-Plas is observed to perform better than the NeQuick is during the high solar activity year 2014, and at the Northern low latitude stations. This better performance is especially observed around the months from February to April and from October to December of 2014. In general, this study reveals that there is a general tendency for the IRI-Plas model to overestimate the GNSS VTEC (especially during low and moderate solar activity periods), and that the IRI-Plas model predictions get better during the high solar activity periods at low latitude stations where the VTECs are relatively enhanced. Fig. 2 also shows that the IRI-Plas overestimations are high during the low solar activity year of 2009, and low during the high solar activity year of 2014. Some underestimations are even observed especially the high latitude stations during the high solar activity year of 2014. The figure shows that there is relatively a better agreement between the NeQuick and GNSS observations during the low and moderate solar activity years of 2006, 2009 and 2012. The NeQuick also typically overestimates the local daytime GNSS observations, but not as much as the IRI-Plas does. The reverse scenario is observed during the high solar activity year of 2014, when the NeQuick typically underestimates the GNSS VTEC.

In a related study in which Ezquer et al. (2017) performed a comparison of the NeQuick and IRI-Plas model for the South American sector using data for June and September 1999 (a year of high solar activity), they observed that the IRI-Plas model performed better than the NeQuick model at the low latitude stations during the month of June, and that the NeQuick performed better at the high latitude stations. This further corroborates our findings that the IRI-Plas model predictions get better during the high solar activity periods at low latitude stations. We however emphasize that our observations do not indicate that IRI-Plas model consistently performs better under these conditions; there are still months (especially around May to August) when the NeQuick performed better than the IRI-Plas.

To lessen the effects introduced by the VTEC magnitudes, we re-illustrated Fig. 5(a) as a function of the percentage annual RMSDs (rather than as a function of the mean annual RMSDs). The result is shown in Fig. 5(b). The percentage annual RMSDs were computed by dividing the mean annual RMSDs by corresponding root-mean-square values of the GNSS observations and then multiplying the result by 100. Fig. 5(b) indicates that, at the low latitude stations, the IRI-Plas percentage annual RMSD profiles typically drop from the low solar activity year of 2009 to the high solar activity year of 2014. For instance at the KAMO station, we observe that the percentage error drops from about 120% in year 2009 to about 30% in 2014. A similar trend is witnessed in all of the other low latitude stations. There is also a somewhat consistent observation in Fig. 7 where the IRI-Plas is specifically observed to perform better than the NeQuick at the low latitude stations during the high solar activity years of 2014/2015 and especially in the equinox months around February/March. These further corroborate our earlier observation that the IRI-Plas model predictions tend to get better during periods of increased solar activity at the low latitude stations (which well represents periods/regions of increased ionospheric ionization). The scenario is probably consequence of the fact that the IRI-Plas overestimates the GNSS VTEC observations. The overestimation does not grow linearly (but slows down) with increased solar activity, so that as the GNSS VTEC observation values are maximally enhanced during the high solar activity periods for the low latitude stations, they eventually catch up with the IRI-Plas prediction values.

To investigate the models during instances of large TEC deviations, electron density profiles (as functions of height) were constructed from the models during instances of large TEC deviations. The first panel (from the left) of Fig. 8 represents the electron density profile for the worst case scenario of the NeQuick (that is for ADIS station in March 2014, which is the station and month in which the NeQuick prediction error was maximum; the RMSE for the NeQuick was 20.95 TECU, while for the IRI-Plas it was 12.97 TECU). The second panel represents the electron density profile for the worst case scenario of the IRI-Plas (that is for THTI station in February 2012; the RMSE for the IRI-Plas was 24.15 TECU, while for the NeQuick it was 11.25 TECU). For reference purposes, the best case scenario of electron density profiles were also included. The third and fourth panels in Fig. 8 respectively represent the best case scenario for the NeQuick (SCOR station in August 2006; NeQuick RMSE = 0.25 TECU and IRI-Plas RMSE = 2.50 TECU) and for the IRI-Plas (RESO station in March 2008; IRI-Plas RMSE = 0.33 TECU and NeQuick RMSE = 2.07 TECU). The profiles in Fig. 8 are shown in the range from 0 to 2000 km; this is the range where the electron densities vary significantly. The profiles illustrated are monthly medians of the local midday profiles. Fig. 8 consistently shows that for each panel, the peak parameters (NmF2 and hmF2) which are used to characterize the profiles are identical. The observed differences are with the methods and equations which are used to construct the profiles from these parameters. As both of these methods have been overwhelmingly validated using electron density measurements from instruments like digisondes, the interest in this work is not to re-examine the methods, but to facilitate the reduction of the model prediction errors by first presenting climatologic assessment of the errors, and subsequently using these error information to adapt the model predictions to empirical observations. There is proposal to use a denser network of GNSS receivers to build surfaces of the model prediction errors in space and time, and to use these surfaces to adapt the model predictions to corresponding GNSS observations. Since one core interest in this study is to motivate increased prediction accuracy for the models, we have presented the results in a manner that the prediction errors can be climatologically modeled (in space and time), and consequently be used to improve the performances of the models.

4. Conclusion

Performances of the NeQuick-2 and IRI-Plas 2017 model for 36 globally distributed stations have been investigated using GNSS VTEC observations for the period from January 2006 to July 2017. Results from the study show that there is a fairly good correlation between the GNSS observations and predictions from both models. The IRI-Plas model is however clearly observed to overestimate the GNSS values, except during the high solar activity years at some high latitude stations. On the other hand, the NeQuick is characteristically observed to underestimate the GNSS values during the high solar activity years. The NeQuick also overestimates the local daytime GNSS observations during the years of low and moderate solar activity, but not as much as the IRI-Plas does.

The VTEC deviations are observed to be highest during the local daytimes as compared to nighttime and early morning values. The VTEC deviations are greatest for the low latitude stations, followed by the middle latitude stations and then least for the high latitude stations. These observations are explained to be due to the tendency for model prediction errors to decrease with lower quantity values and vice versa. The low latitudes are also explained to be prone to several anomalous ionospheric phenomena that make the ionosphere in the region difficult to predict.

At the low latitude stations, the VTEC deviations are greater during the equinox months than during the solstice months. At the Northern high latitudes, the VTEC deviations are greatest around the month of June (northern summer), while at the Southern high latitudes the deviations are greatest around the months of December/January (southern summer). The increased prediction errors are also explained to be associated with increased ionospheric ionization levels (and so increased VTEC values) at those seasons for the regions.

In particular, the IRI-Plas model predictions were observed to get better during periods of increased solar activity at the low latitude stations; the model's percentage error drops from higher values during lower solar activity years to lower values during higher solar activity years.

In overall, the NeQuick prediction errors were observed to be less than the IRI-Plas prediction errors; the mean annual errors for the IRI-Plas predictions are typically observed to increase from about 3 TECU at the high latitude stations to about 12 TECU at the low latitude stations, while typical annual prediction errors for the NeQuick go from about 2 TECU at the high latitudes to about 7 TECU at the low latitudes. There are however certain stations (e.g. DAV1, KERG, and ADIS) where the IRI-Plas predictions are observed to be better than the NeQuick predictions. Out of a total 4497 months in which GNSS data was available for all the stations put together for the entire period covered in this work, the NeQuick model was observed to perform better in 83% of the months while the IRI-Plas performed better in 17% of the months.

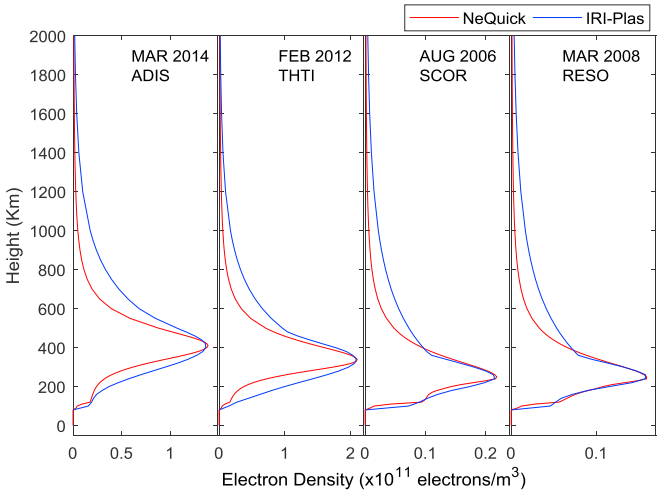

Fig. 8. Electron density profiles for worst case scenarios of the NeQuick and IRI-Plas (first and second panels) and for their respective best case scenarios (third and fourth panels).

Acknowledgement

We immensely appreciate supports provided by the CV Raman International Fellowship (DST/INT/CVRF/2016), the Center for Atmospheric Research, and the Indian Institute for Geomagnetism. We also appreciate developers of the IRI-Plas Model and the NeQuick for making their models available. We thank providers of the University of California, San Diego (UCSD) network of GNSS receivers for making data from the network available.

References

Adebiyi, S.J., Adimula, I.A., Oladipo, O.A., Joshua, B.W., 2016. Assessment of IRI and IRI-Plas models over the African equatorial and low-latitude region. J. Geophys. Res. 121, 7287–7300. https://doi.org/10.1002/2016JA022697.

Arikan, F., Seymur, S., Hakan, T., Orhan, A., Gulyaeva, T.L., 2016. Performance of GPS slant total electron content and IRI-Plas-STEC for days with ionospheric disturbance. Geodesy and Geodynamics 7 (1), 1–10.

Bailey, G.J., Balan, N., Su, Y.Z., 1997. The Sheffield University plasmasphere ionosphere model-a review. J. Atmos. Sol. Terr. Phys. 59 (13), 1541–1552.

Bidaine, B., Warnant, R., 2010. Assessment of the NeQuick model at mid-latitudes using GNSS TEC and ionosonde data. Adv. Space Res. 45 (9), 1122–1128.

Bilitza, D., 1990. International Reference Ionosphere 1990. National Space Science Data Center 90-22, Greenbelt Maryland.

Bilitza, D., Reinisch, B.W., 2008. International reference ionosphere 2007 improvements and new parameters. Adv. Space Res. 42 (4), 599–609.

Bolaji, O.S., Oyeyemi, E.O., Adewale, A.O., Wu, Q., Okoh, D., Doherty, P.H., Kaka, R.O., Abbas, M., Owolabi, C., Jidele, P.A., 2017. Assessment of IRI-2012, NeQuick-2 and

IRI-Plas 2015 models with observed equatorial ionization anomaly in Africa during 2009 sudden stratospheric warming event. J. Atmos. Sol. Terr. Phys. 164, 203–214.
Buresova, D., Cander, L.R., Vernon, A., Zolesi, B., 2006. Effectiveness of the IRI-2001-predicted N(h) profile updating with real-time measurements under intense geomagnetic storm conditions over Europe. Adv. Space Res. 37 (5), 1061–1068.
Chiu, Y.T., 1975. An improved phenomenological model of ionospheric density. J. Atmos. Terr. Phys. 37, 1563–1570.
Coïsson, P., Radicella, S.M., Leitinger, R., Nava, B., 2006. Topside electron density in IRI and NeQuick: features and limitations. Adv. Space Res. 37, 937–942.
Di Giovanni, G., Radicella, S.M., 1990. An analytical model of the electron density profile in the ionosphere. Adv. Space Res. 10 (11), 27–30.
Ezquer, R.G., de Adler, N.O., Heredia, T., 1994. Predicted and measured total electron content at both peaks of the equatorial anomaly. Radio Sci. 29, 831–838.
Ezquer, R.G., Scida, L.A., Orue, Y.M., Nava, B., Cabrera, M.A., Brunini, C., 2017. NeQuick 2 and IRI Plas VTEC predictions for low latitude and South American sector. Adv. in Space Res. https://doi.org/10.1016/j.asr.2017.10.003.
Gulyaeva, T.L., Huang, X., Reinisch, B.W., 2002. Plasmaspheric extension of topside electron density profiles. Adv. Space Res. 29 (6), 825–831.
Gulyaeva, T.L., Bilitza, D., 2012. Towards standard earth ionosphere and plasmasphere model. In: Larsen, R.J. (Ed.), New Developments in the Standard Model. Nova Science Publishers, pp. 1–39.
Habarulema, J.B., 2010. A Contribution to TEC Modelling over Southern Africa Using GPS Data [PhD Thesis]. Rhodes University.
Hochegger, G., Nava, B., Radicella, S.M., Leitinger, R., 2000. A family of ionospheric models for different uses. Phys. Chem. Earth 25 (4), 307–310.
Huba, J.D., Joyce, G., Fedder, J.A., 2000. Sami2 is Another Model of the Ionosphere (SAMI2) - a new low-latitude ionosphere model. J. Geophys. Res. 105 (A10), 23035–23053.
Jin, S.G., Park, J.U., 2007. GPS ionospheric tomography: a comparison with the IRI-2001 model over South Korea. Earth Planets Space 59, 287–292.
Jin, S.G., Park, J., Wang, J., Choi, B., Park, P., 2006. Electron density profiles derived from ground-based GPS observations. J. Navig. 59 (3), 395–401. https://doi.org/10.1017/S0373463306003821.
Jin, S.G., Cho, J., Park, J., 2007. Ionospheric slab thickness and its seasonal variations observed by GPS. J. Atmos. Sol. Terr. Phys. 69 (15), 1864–1870. https://doi.org/10.1016/j.jastp.2007.07.008.
Jin, S.G., Najibi, N., 2014. Sensing snow height and surface temperature variations in Greenland from GPS reflected signals. Adv. Space Res. 53 (11), 1623–1633. https://doi.org/10.1016/j.asr.2014.03.005.
Jin, S.G., Wang, J., Zhang, H., Zhu, W.Y., 2004. Real-time monitoring and prediction of the total ionospheric electron content by means of GPS observations. Chin. Astron. Astrophys. 28 (3), 331–337. https://doi.org/10.1016/j.chinastron.2004.07.008.
Jodogne, J.C., Nebdi, H., Warnant, R., 2005. GPS TEC and ITEC from digisonde data compared with NeQuick model. Adv. Radio. Sci. 2 (11), 269–273.
Klobuchar, J.A., 1996. Ionospheric effects on GPS. In: Parkinson, B.W., Spilker, J.J. (Eds.), Global Positioning System: Theory and Applications 2, Progress in Astronautics and Aeronautics, p. 164.
Leitinger, R., Zhang, M.L., Radicella, S.M., 2005. An improved bottomside for the ionospheric electron density model NeQuick. Ann. Geophys. 48 (3), 525–534.
Maltseva, O.A., Zhbankov, G.A., Mozhaeva, N.S., 2013. Advantages of the new model of IRI (IRI-Plas) to simulate the ionospheric electron density: case of the European area. Adv. Radio. Sci. 11, 307–311.
McKinnell, L.A., Opperman, B.D.L., Cilliers, P.J., 2007. GPS TEC and ionosonde TEC over Grahamstown, South Africa: first comparisons. Adv. Space Res. 39 (5), 816–820.
Nava, B., Coïsson, P., Radicella, S.M., 2008. A new version of the NeQuick ionosphere electron density model. J. Atmos. Sol. Terr. Phys. 70 (15), 1856–1862.
Nava, B., Radicella, S.M., 2014. The NeQuick model: characteristics and uses. In: IGS Workshop, Pasadena, 23–27 June 2014.
Okoh, D.I., Eze, A.C., Adedoja, O., Okere, B., Okeke, P., 2012. A comparison of IRI-TEC predictions with GPS-TEC measurements over Nsukka, Nigeria. Space Weather 10, S10002.
Okoh, D., McKinnel, L.A., Cilliers, P., Okere, B., Okonkwo, C., Rabiu, B., 2015. IRI-vTEC versus GPS-vTEC for Nigerian SCINDA GPS stations. Adv. Space Res. 55, 1941–1947.
Okoh, D., Owolabi, O., Ekechukwu, C., Folarin, O., Arhiwo, G., Agbo, J., Bolaji, S., Rabiu, B., 2016. A regional GNSS-VTEC model over Nigeria using neural networks: a novel approach. Geodesy & Geodynamics 7 (1), 19–31. https://doi.org/10.1016/j.geog.2016.03.003.
Rabiu, A.B., Groves, K., Abdulrahim, R.B., Fayose, R.S., Adeniyi, J.O., Ariyibi, E.A., Oyeyemi, E.O., Okere, B.I., 2011. TEC Derived from some GPS Stations in Nigeria and comparison with the IRI. In: United Nations International Meeting on the Applications of GNSS, 12–16, December, Vienna, Austria.
Rabiu, A.B., Adewale, A.O., Abdulrahim, R.B., Oyeyemi, E.O., 2014. TEC derived from some GPS stations in Nigeria and comparison with the IRI and Nequick models. Adv. Space Res. 53 (9), 1290–1303. https://doi.org/10.1016/j.asr.2014.02.009.
Radicella, S.M., Leitinger, R., 2001. The evolution of the DGR approach to model electron density profiles. Adv. Space Res. 27, 35–40. https://doi.org/10.1016/S0273-1177(00)00138-1.
Radicella, S.M., Zhang, M.L., 1995. The improved DGR analytical model of electron density height profile and total electron content in the ionosphere. Ann. Geofisc. 38 (1), 35–41.
Rama Rao, P.V.S., Gopi, K.S., Niranjan, K., Prasad, S.V.V.D., 2006. Temporal and spatial variations in TEC using simultaneous measurements from the Indian network of receivers during the low solar activity period of 2004–2005. Ann. Geophys. 24, 3279–3292.
Roble, R.G., Ridley, E.C., Richmond, A.D., 1988. A coupled thermosphere/ionosphere general circulation model. Geophys. Res. Lett. 15 (12), 1325–1328.
Seemala, G., Delay, S., 2010. GNSS TEC data processing, 2nd satellite navigation science and technology for Africa. In: ICTP Trieste, Italy, 6–24 April 2010.
Seemala, G.K., Valladares, C.E., 2011. Statistics of total electron content depletions observed over the South American continent for the year 2008. Radio Sci. 46, RS5019. https://doi.org/10.1029/2011RS004722.
Wang, N., Yuan, Y., Li, Z., Li, Y., Huo, X., Li, M., 2017. An examination of the Galileo NeQuick model: comparison with GPS and JASON TEC. GPS Solut. 21, 605–615. https://doi.org/10.1007/s10291-016-0553-x.
Zakharenkova, I.E., Cherniak, I.V., Krankowski, A., Shagimuratov, I.I., 2015. Vertical TEC representation by IRI 2012 and IRI Plas models for European midlatitudes. Adv. Space Res. 55, 2070–2076. https://doi.org/10.1016/j.asr.2014.07.027.